



The sensor kinase MtrB of *Mycobacterium tuberculosis* regulates hypoxic survival and establishment of infection

Received for publication, May 23, 2019, and in revised form, October 24, 2019. Published, Papers in Press, October 25, 2019, DOI 10.1074/jbc.RA119.009449

Srijan Kaushik Banerjee^{†1,2}, Suruchi Lata^{†1}, Arun Kumar Sharma^{†1}, Shreya Bagchi[†], Manish Kumar^{†3}, Sanjaya Kumar Sahu^{†4}, Debasree Sarkar^{§5}, Pushpa Gupta[¶], Kuladip Jana^{||}, Umesh Datta Gupta[¶], Ramandeep Singh^{**}, Sudipto Saha[§], Joyoti Basu^{†6,7}, and Manikuntala Kundu^{†6,8}

From the [†]Department of Chemistry, Bose Institute, Kolkata 700009, India, [§]Divisions of Bioinformatics and ^{||}Molecular Medicine, Bose Institute, Kolkata 700054, India, [¶]National JALMA Institute for Leprosy and Other Mycobacterial Diseases, Tajganj, Agra 282004, India, and ^{**}Vaccine and Infectious Disease Research Centre, Translational Health Science and Technology Institute, NCR-Biotech Science Cluster, 3rd Milestone, Faridabad–Gurgaon Expressway, Faridabad, Haryana 121001, India

Edited by Chris Whitfield

Paired two-component systems (TCSs), having a sensor kinase (SK) and a cognate response regulator (RR), enable the human pathogen *Mycobacterium tuberculosis* to respond to the external environment and to persist within its host. Here, we inactivated the SK gene of the TCS MtrAB, *mtrB*, generating the strain $\Delta mtrB$. We show that *mtrB* loss reduces the bacterium's ability to survive in macrophages and increases its association with autophagosomes and autolysosomes. Notably, the $\Delta mtrB$ strain was markedly defective in establishing lung infection in mice, with no detectable lung pathology following aerosol challenge. $\Delta mtrB$ was less able to withstand hypoxic and acid stresses and to form biofilms and had decreased viability under hypoxia. Transcriptional profiling of $\Delta mtrB$ by gene microarray analysis, validated by quantitative RT-PCR, indicated down-regulation of the hypoxia-associated *dosR* regulon, as well as genes associated with other pathways linked to adaptation of *M. tuberculosis* to the host environment. Using *in vitro* biochemical assays, we demonstrate that MtrB interacts with DosR (a noncognate RR) in a phosphorylation-independent manner. Electrophoretic mobility shift assays revealed that MtrB enhances the binding of DosR to the *hspX* promoter, suggesting an unexpected role of MtrB in DosR-regulated gene expression in *M. tuberculosis*. Taken together, these findings indicate that MtrB functions as a regulator of DosR-dependent gene expres-

sion and in the adaptation of *M. tuberculosis* to hypoxia and the host environment. We propose that MtrB may be exploited as a chemotherapeutic target against tuberculosis.

The ability of *Mycobacterium tuberculosis* to remain dormant within its host for extended periods of time without eliciting any obvious symptoms of disease, its ability to relapse once drug treatment is withdrawn (1), and the lack of an efficacious vaccine pose a threat to worldwide efforts to control the disease, necessitating efforts to identify new therapeutic strategies. Two-component systems (TCSs)⁹ are involved in stimulus-dependent adaptation of bacteria to their environment. Canonical, paired TCSs comprise a membrane-bound sensor kinase (SK) and a cytosolic response regulator (RR). A phosphotransfer relay is activated when the SK senses a stimulus, culminating in phosphorylation of the cognate RR. TCSs regulate bacterial virulence, pathogenesis, biofilm formation, cell division, and metabolite production, to name a few functions. *M. tuberculosis* has 12 paired TCSs, six orphan RRs, and two orphan SKs (2). The *mtrA*–*mtrB* TCS is present in all mycobacterial species characterized (3). *mtrA*, the RR, is essential in *M. tuberculosis*. In *Mycobacterium smegmatis*, MtrB, the SK, localizes to the septa and the poles in a phosphorylation-dependent manner (4) to regulate the expression of the MtrA targets *ripA*, *fbpB*, and *ftsI* (5).

In high-G+C Gram-positive bacteria, MtrAB has been suggested to be the functional analog of the YycFG system in low GC-containing Gram-positive bacteria (6, 7). Similar to YycF in *Bacillus subtilis*, MtrA is the only response regulator of TCS, known to be essential in *Mycobacterium* (3). YycFG controls multiple cellular pathways linked to cell wall synthesis, cell growth, and cell division (8). Mutations in this TCS alter cell

This work was supported in part by Science and Engineering Research Board Grant EMR/2015/001154 (to J. B. and M. Kundu) and J. C. Bose Fellowship SB/S2/JCB-049/2016 (to J. B.). The authors declare that they have no conflicts of interest with the contents of this article.

This article contains Figs. S1–3 and Tables S1–S6.

The data discussed in this publication have been deposited in NCBI's Gene Expression Omnibus and are accessible through GEO Series accession number GSE97958.

¹ These authors made equal contributions to this work.

² Present address: Dept. of Microbiology and Immunology, University of Arkansas for Medical Sciences, Little Rock, AR 72205.

³ Present address: Laboratory of Host-Pathogen Dynamics, NHLBI, National Institutes of Health, Bethesda, MD 20892.

⁴ Present address: Dept. of Internal Medicine and Nephrology Division, Washington University, St. Louis, MO 63110.

⁵ Present address: Dept. of Urology, SUNY Upstate Medical University, Syracuse, NY 13202.

⁶ Both authors should be considered joint senior authors.

⁷ To whom correspondence may be addressed. Tel.: 91-33-23031153; E-mail: joyotibas@gmail.com.

⁸ To whom correspondence may be addressed. E-mail: manikuntala.kundu@gmail.com.

⁹ The abbreviations used are: TCS, two-component system; SK, sensor kinase; RR, response regulator; cfu, colony-forming unit(s); TAG, triacylglycerol; EMSA, electrophoretic mobility shift assay; DCW, division cell wall; BMDM, bone marrow-derived macrophage; TNF, tumor necrosis factor; IL, interleukin; pd, protein-DNA; pp, protein-protein; qRT-PCR, quantitative RT-PCR; NTA, nitrilotriacetic acid; M-PFC, mycobacterial protein fragment complementation; ESCRT, endosomal sorting complex required for transport; ADC, bovine albumin, dextrose, and catalase; m.o.i., multiplicity of infection; DHFR, dihydrofolate reductase; TRIM, trimethoprim; MB, Middlebrook.

wall permeability, antibiotic resistance, biofilm formation, cellular morphology, osmotic stress, and virulence of pathogenic bacteria (9). Similar to YycFG, alterations in MtrAB expression also affect cell wall, cell division, and cellular morphology in *Mycobacterium* and *Corynebacterium* (4, 10, 11).

The foregoing preamble suggests that MtrB could be a regulator of cell wall synthesis, cellular morphology, biofilm formation, and survival of *M. tuberculosis* in vivo. To explore this, we inactivated *mtrB* in *M. tuberculosis* to generate the $\Delta mtrB$ strain. Inactivation of *mtrB* renders the bacilli unable to withstand hypoxia and acid stress. $\Delta mtrB$ is unable to form biofilms, possibly due to defective ketomycolic acid biosynthesis. The inability of $\Delta mtrB$ to survive under hypoxia is linked to dramatic down-regulation of the *dosR*–*dosS* regulon. Its response regulator DosR is induced in response to hypoxia and enables recovery from dormancy. Based on the relative transcription levels observed during progression of cells toward stationary phase *in vitro*, we hypothesized that the compromised transcription of the *dosR* regulon is directly associated with the inability of the bacteria to launch a response to hypoxia in the absence of *mtrB*. We confirmed direct interaction of MtrB with the noncognate response regulator DosR. MtrB enhanced binding of DosR with its targets, suggesting that in addition to its role as a sensor kinase, MtrB could exert MtrA-independent functions. Reduced transcription of *dosR*-regulated genes early during infection is likely to be linked to compromised survival of $\Delta mtrB$ in macrophages. The global changes in the bacterial transcriptome in the absence of *mtrB* could possibly explain the attenuated phenotype of $\Delta mtrB$ in a mouse model of infection with no visible granuloma formation. In summary, our results establish a previously unrecognized, central regulatory role of MtrB in the pathogenesis of *M. tuberculosis*. Therefore, MtrB could be exploited to develop novel therapeutics for the management of tuberculosis.

Results

M. tuberculosis MtrB is required to maintain growth, cell size, and surface architecture

To gain insight into the role of MtrB, we inactivated *mtrB* ($\Delta mtrB$) of *M. tuberculosis* by disrupting the *mtrB* gene with a kanamycin cassette. PCR products of the expected size were obtained for the wildtype (WT) and $\Delta mtrB$ (Fig. S1, A–C). Southern blotting further confirmed the inactivation of *mtrB* (Fig. S1, D and E). PCR using genomic DNA as template confirmed the presence of *mtrA* in both the WT and $\Delta mtrB$ (Fig. S1F). The growth of $\Delta mtrB$ was retarded compared with the WT (Fig. 1A). This could be reversed upon complementation with *mtrB* ($\Delta mtrB::mtrB$), suggesting that the growth retardation was specifically attributable to *mtrB*. Complementation of *mtrB* was confirmed by immunoblotting with MtrB antibody (Fig. S1G). $\Delta mtrB$ showed increased aggregation when grown in liquid medium containing Tween 80 for 10 min (Fig. 1B). The presence of Tween 80 did not affect the viability of the bacteria (Fig. S1H). This was reversed in $\Delta mtrB::mtrB$. When grown on solid medium, $\Delta mtrB$ displayed altered colony morphology compared with the WT *M. tuberculosis* (Fig. 1C). This was reversed upon complementation with *mtrB*. Altered colony

morphology of *M. tuberculosis* has been linked to alterations in cell wall synthesis (12).

The pole-to-pole length of exponentially growing $\Delta mtrB$ was significantly greater than that of the WT *M. tuberculosis*. When evaluated by scanning EM, the average cell length of 30 bacteria was observed to be $\sim 2 \mu\text{m}$ for the WT, whereas it was $\sim 3 \mu\text{m}$ for $\Delta mtrB$ (Figs. 1D and S1I). These phenotypic changes suggested that MtrB possibly regulates cell division in *M. tuberculosis*. The length was restored in $\Delta mtrB::mtrB$.

MtrB is required for biofilm formation

M. tuberculosis observed in infected guinea pigs after drug treatment or in certain caseating lesions in humans exhibits biofilm-like architecture (13). In view of this, we tested whether the absence of *mtrB* alters the ability of the bacterium to form biofilms. Strikingly, $\Delta mtrB$ was not able to form biofilms (Fig. 1E), whereas biofilm formation was restored in $\Delta mtrB::mtrB$. MtrB is therefore required for biofilm formation in *M. tuberculosis*. We further tested whether the influence of MtrB on biofilm formation depends on MtrA. To do so, we introduced a gain-of-function mutant of MtrA, MtrA(Y102C), in $\Delta mtrB$. This variant of MtrA functions even in the absence of MtrB (4, 14). The overexpression of His-tagged MtrA(Y102C) was confirmed by immunoblotting with His antibody (Fig. S1J). Biofilm formation could not be restored upon introduction of MtrA(Y102C) in $\Delta mtrB$ (Fig. 1E), suggesting that MtrB-dependent biofilm formation in *M. tuberculosis* probably occurs independently of MtrA. *M. tuberculosis* biofilms are rich in mycolic acids (15). We performed a qualitative analysis of mycolates in the WT strain and $\Delta mtrB$. *M. tuberculosis* H37Rv is characterized by the presence of three major classes of mycolic acids, α , methoxy, and keto (Fig. 1F, second lane from left). $\Delta mtrB$ was compromised in ketomycolate formation compared with the WT (Fig. 1F, third lane from left), and this was rescued by complementation with *mtrB* (Fig. 1F, first lane from left). Pellicle biofilm formation in *M. tuberculosis* requires ketomycolates (16), suggesting that a deficiency of ketomycolates in $\Delta mtrB$ could be associated with compromised biofilm formation.

MtrB is required for survival under acid stress and hypoxia

Within the host, *M. tuberculosis* encounters a hostile environment to which it must respond appropriately to survive. Among the hostile conditions is the acidic pH of the phagosome or phagolysosome. We tested whether $\Delta mtrB$ is competent to withstand acid stress. The percent reduction of growth at pH 5.5 relative to growth at pH 7.0 was significantly higher for $\Delta mtrB$ compared with the WT after 4 or 6 days of exposure to pH 5.5 (Fig. 1G). This effect was reversed in the *mtrB*-complemented strain. Complementation of $\Delta mtrB$ with MtrA(Y102C) mutant did not reverse the acid sensitivity of the mutant (Fig. 1H), suggesting that the role of MtrB in aiding the bacterium to withstand acid stress is independent of MtrA. Wide-ranging remodeling of the transcriptome is associated with the entry of *M. tuberculosis* into a dormant state when it encounters hypoxia. In view of this, we tested the ability of $\Delta mtrB$ to withstand hypoxia. Hypoxic conditions were generated in sealed tubes, and the viability of the bacterium was evaluated by determination of cfu at different periods of time. Although WT and

MtrB regulates mycobacterial survival in vivo

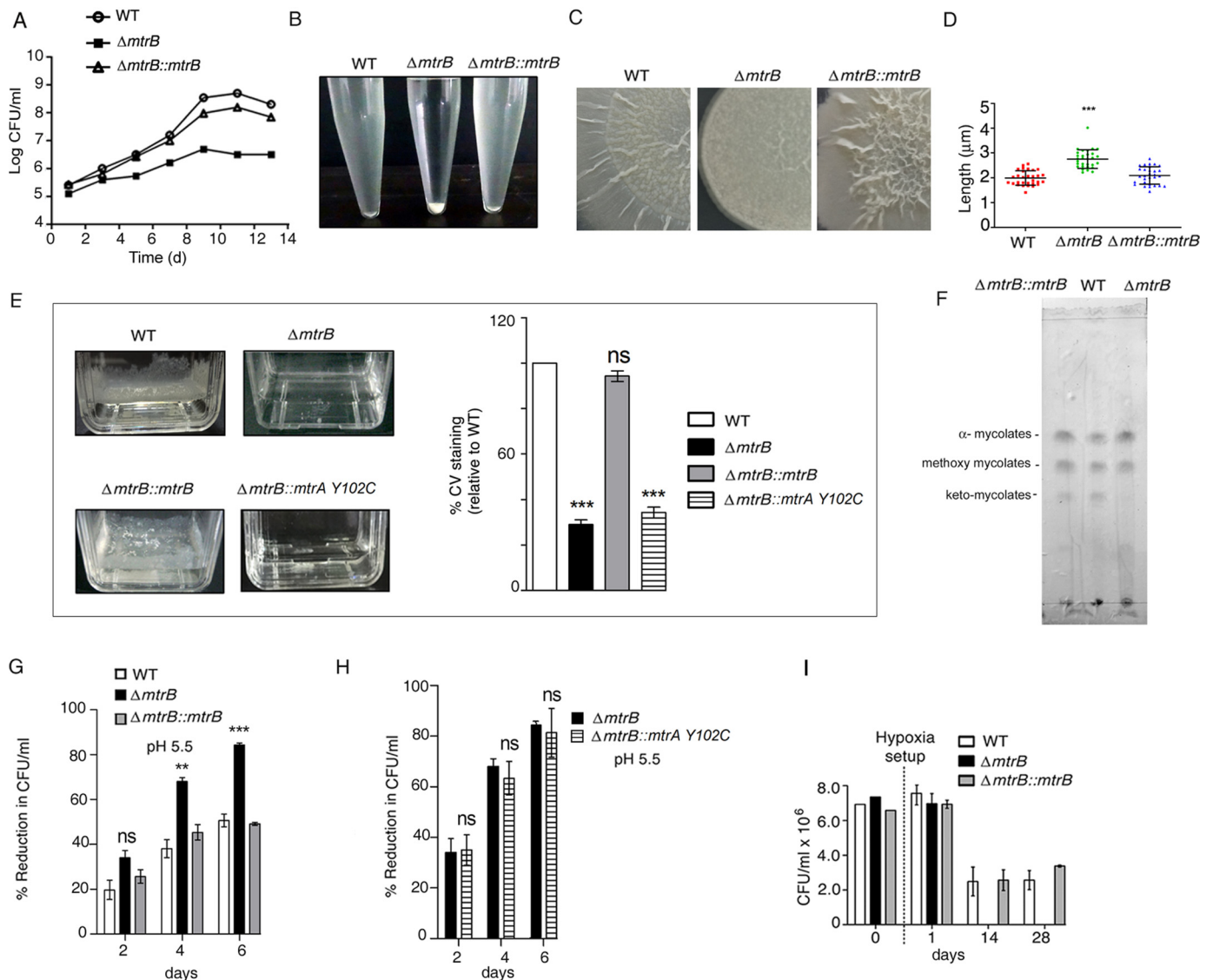


Figure 1. *M. tuberculosis* requires MtrB to maintain growth, cell size, surface integrity, biofilm formation, and survival under acid stress and hypoxia. A, growth curve of WT, $\Delta mtrB$, and $\Delta mtrB::mtrB$ strains monitored by recording the cfu over a period of time in days (d). B, aggregation of WT, $\Delta mtrB$, and $\Delta mtrB::mtrB$ strains observed after keeping growing cultures standing for 10 min. C, colony morphology of WT, $\Delta mtrB$, and $\Delta mtrB::mtrB$ strains. D, scanning EM analyses of cell lengths of WT, $\Delta mtrB$, and $\Delta mtrB::mtrB$ strains. Pole-to-pole lengths of 30 bacteria from at least five fields for each strain were measured. ***, $p < 0.001$. E, biofilm formation of WT, $\Delta mtrB$, $\Delta mtrB::mtrB$, and $\Delta mtrB::mtrA(Y102C)$ strains after 6 weeks of incubation. The right-hand panel indicates percentage of crystal violet (CV) taken up by biofilms of different strains compared with WT. Error bars represent S.D., $n = 3$. ***, $p < 0.001$; **, $p < 0.01$; ns, nonsignificant. F, survival of *M. tuberculosis* strains after recovery from hypoxia. After establishment of hypoxia, cfu were determined at the indicated time intervals. No colonies were obtained for $\Delta mtrB$ kept in hypoxic conditions for 14 or 28 days. Images in B, C, E, and F are representative of at least two independent experiments.

$\Delta mtrB::mtrB$ could grow when cells were replated on fresh medium after 14 or 28 days under hypoxia, no colonies were obtained for $\Delta mtrB$ at the same time points (Fig. 1I). These results strongly suggested that MtrB is required for mounting a response that enables bacteria to withstand hypoxia.

MtrB is required for survival of *M. tuberculosis* in macrophages

The observed changes in phenotypic behavior of $\Delta mtrB$ compared with the WT suggested that MtrB could be a likely regulator of the fate of *M. tuberculosis* during infection. To test whether MtrB has a role during infection *ex vivo*, we tested the

ability of $\Delta mtrB$ to survive in bone marrow–derived macrophages (BMDMs). Loss of *mtrB* compromised the ability of the bacterium to survive in macrophages (Fig. 2A). This was reversed upon complementation of the mutant with *mtrB*. *M. tuberculosis* escapes lysosomal killing by subverting xenophagy (17). We tested whether attenuated survival of $\Delta mtrB$ within macrophages could be attributed to its increased association with autophagosomes and trafficking to lysosomes. Colocalization of the bacteria with LC3 was used as a method of analyzing association of bacteria with autophagosomes, whereas colocalization of the bacteria with LAMP1 was used to monitor trafficking of bacteria to lysosomes.

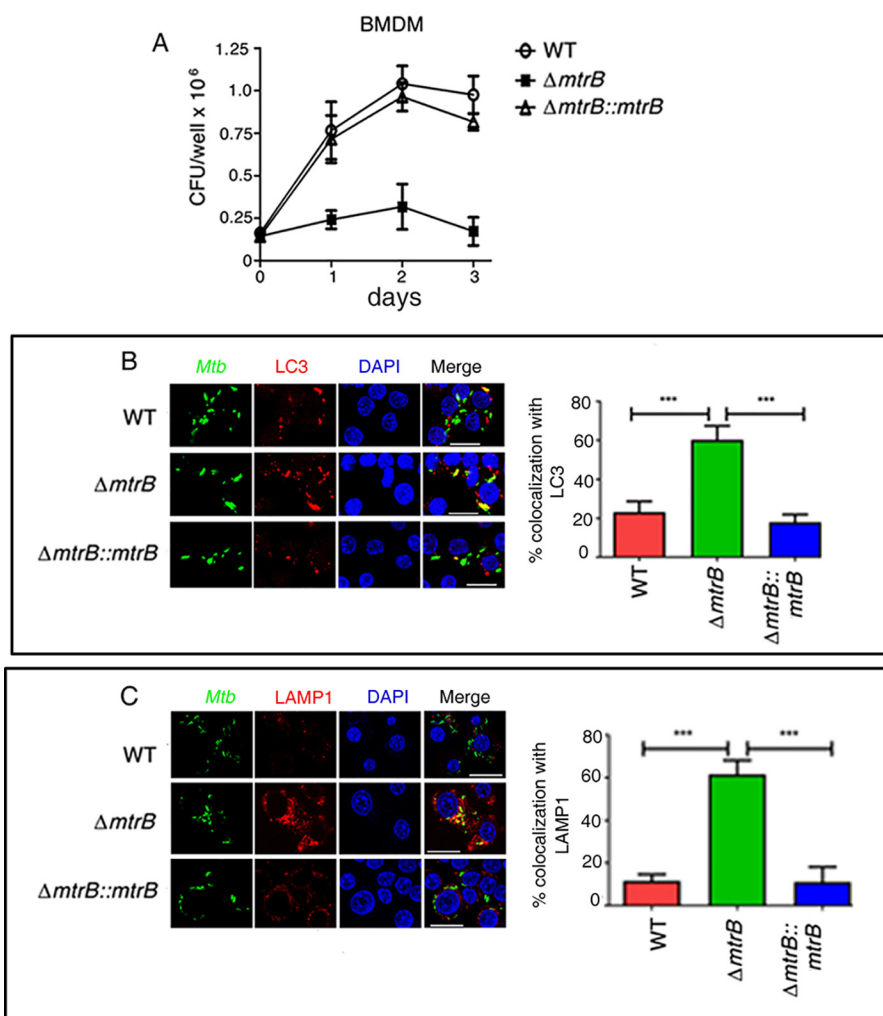


Figure 2. MtrB is required for the survival of *M. tuberculosis* in macrophages and for trafficking to autophagosomes and lysosomes. *A*, survival of WT *M. tuberculosis*, $\Delta mtrB$, and $\Delta mtrB::mtrB$ in BMDMs. Infected cells were lysed, and bacterial survival was determined by enumerating cfu. $\Delta mtrB$ was compromised for survival in macrophages compared with the WT. This was rescued by complementation with *mtrB*. *B* and *C*, BMDMs were infected with FITC-labeled *M. tuberculosis* (WT, $\Delta mtrB$, or $\Delta mtrB::mtrB$), fixed, and immunolabeled with anti-LC3 (*B*) or anti-LAMP1 (*C*) followed by Alexa Fluor 546-conjugated secondary antibody. Cells were stained with 4',6-diamidino-2-phenylindole (DAPI) to visualize the nuclei. Scale bars, 20 μ m. *B* and *C*, representative images from three independent experiments. Percent colocalization of each of the three strains with LC3 (*B*) or LAMP1 (*C*) was calculated by counting at least 100 bacteria from five different fields. Error bars represent S.D. $n = 3$. ***, $p < 0.001$.

FITC-labeled $\Delta mtrB$ colocalized at a significantly higher percentage than the WT with Alexa Fluor 546-labeled LC3B in BMDMs (Fig. 2*B*), suggesting that $\Delta mtrB$ was impaired in its ability to escape xenophagy compared with the WT. Furthermore, a larger percentage of FITC-labeled $\Delta mtrB$ colocalized with Alexa Fluor 546-labeled LAMP1 compared with the WT (Fig. 2*C*), suggesting increased trafficking to lysosomes and arguing in favor of a role of MtrB in blocking phagosome-lysosome fusion as well as bacterial survival in macrophages.

MtrB is required for establishing infection in mice

The reduced capability of $\Delta mtrB$ to survive in macrophages prompted us to test its ability to survive *in vivo*. Mice were infected with the WT or $\Delta mtrB$ via the aerosol route. Although the initial loads of both strains were the same (~ 100 bacilli in the lungs), the cfu recovered from infected lungs decreased significantly over time in the case of $\Delta mtrB$ (Fig. 3*A*), suggesting a compromised ability of the mutant to replicate in the lungs. The WT *M. tuberculosis* disseminated to the spleens of infected

mice (Fig. 3*B*), whereas for $\Delta mtrB$, significantly less bacteria were recovered from the spleens after 12 and 14 weeks of infection (Fig. 3*B*). Splenomegaly was observed in mice infected with WT *M. tuberculosis* where the average length of the spleen was ~ 2.8 cm, whereas spleens from mice infected with $\Delta mtrB$ were of an average length of ~ 1.5 cm (Fig. 3*C*). During infection, *M. tuberculosis* persists within granulomas where it is shielded from the antimycobacterial immune effectors of the host. Histopathological evaluation showed that WT *M. tuberculosis*-infected lung sections displayed granulomas, whereas no granulomas were observed in $\Delta mtrB$ -infected lung sections (Fig. 3*D*). We conclude that the absence of *mtrB* is associated with an attenuated phenotype of the bacterium and an absence of immunopathology in the lung comparable with the WT strain in infected mice.

MtrB regulates the cytokine response during infection

Considering the attenuation of $\Delta mtrB$ as well as the absence of immunopathology in the mouse lung infected with $\Delta mtrB$,

MtrB regulates mycobacterial survival in vivo

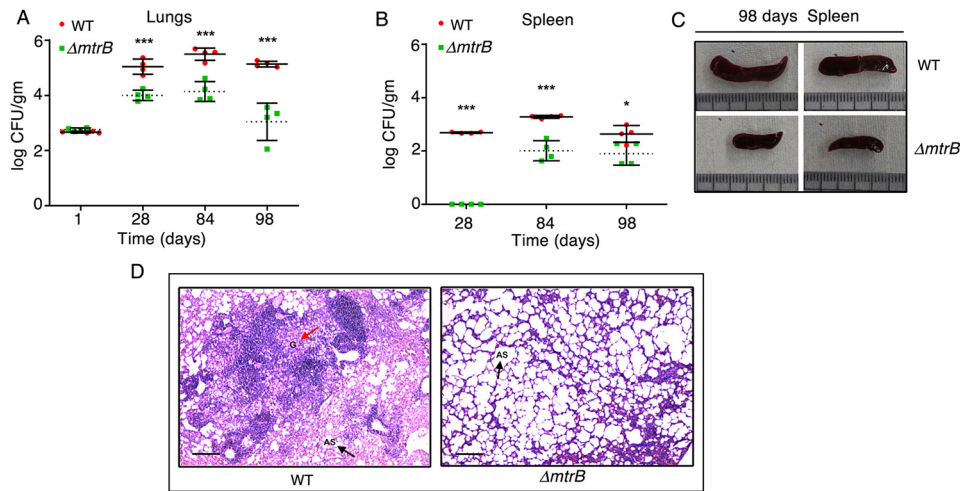


Figure 3. MtrB is required to establish active infection in mice. A and B, survival of the WT *M. tuberculosis* or $\Delta mtrB$ strains in the lungs (A) or spleen (B) of mice after aerosol infection with ~ 100 bacilli/lung. Error bars represent S.D. and the means of cfu obtained with four animals per strain from one experiment. ***, $p < 0.001$; *, $p < 0.05$. C, sizes of the spleens from two individual mice infected with either WT or $\Delta mtrB$ for 14 weeks. Scale, 3 cm. Images are representative of one experiment with four animals per strain. D, histopathology of lung sections collected after 12 weeks of infection with the indicated strains. Sections were stained with hematoxylin and eosin and observed under a light microscope at $40\times$ magnification. G denotes granuloma (red arrow), and AS (black arrow) denotes alveolar space. Images are representative of one experiment with four animals per strain. Scale bar, $10\ \mu\text{m}$.

we tested the expression of cytokines both *ex vivo* and *in vivo*. The release of proinflammatory cytokines TNF α and IL-6 were lower in the case of BMDMs infected with $\Delta mtrB$ compared with the WT (Fig. S2). This was reversed in $\Delta mtrB::mtrB$. Similar to the results observed *ex vivo*, $\Delta mtrB$ elicited lower expression of *Tnfa* and *Il6* in the lungs of infected mice (Fig. S2). These results were in harmony with the lack of immunopathology in the lungs of mice infected with $\Delta mtrB$.

Transcriptome analysis shows perturbation of important pathways, processes, and nodes in the transcriptional network in $\Delta mtrB$

To gain insights into the role of MtrB in regulating morphology, growth behavior, biofilm formation, and survival of *M. tuberculosis* within its host, we performed genome-wide transcriptional profiling of the WT and $\Delta mtrB$. System-level analyses of the transcriptome showed that 1,014 genes were differentially expressed in $\Delta mtrB$. 551 of these 1,014 genes were up-regulated in the mutant, whereas 463 genes were down-regulated. The differentially regulated processes were mapped according to their functions annotated in TubercuList <https://mycobrowser.epfl.ch/> (57).¹⁰ Strikingly, a large number of genes down-regulated in $\Delta mtrB$ mapped to crucial functions/processes associated with cell wall biosynthesis/cell division, central carbon metabolism/respiration, and the response to hypoxia (Fig. 4, A and B). For the sake of clarity, we will focus on these down-regulated genes in this report.

Within its host, *M. tuberculosis* resides in acidic compartments such as the macrophage or the caseum of a necrotic granuloma. This requires sensing and responding to the acidic environment. A large number of genes are up-regulated when *M. tuberculosis* senses acidic pH or the phagosomal environment of macrophages. To obtain information on whether

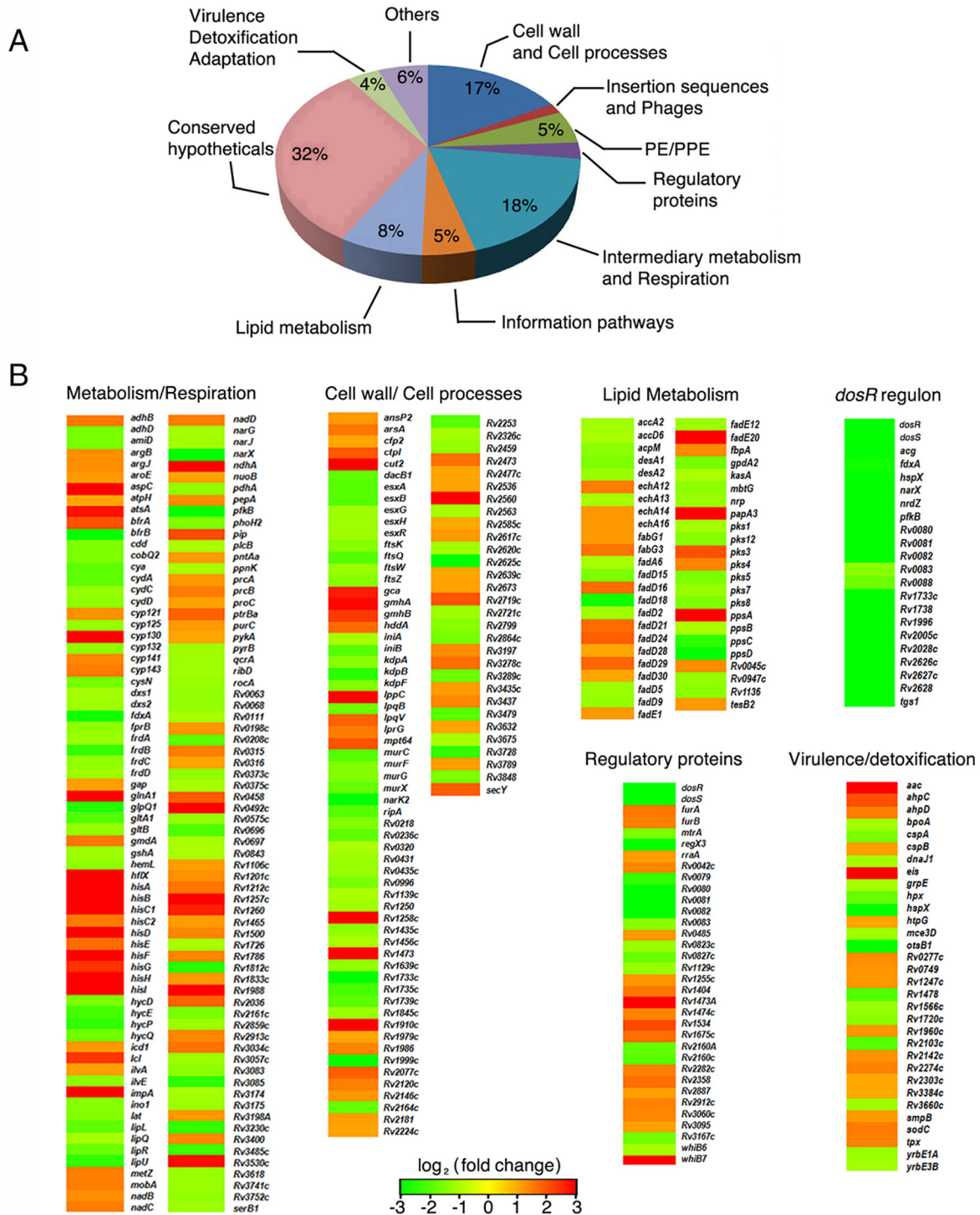
altered gene expression of $\Delta mtrB$ could possibly compromise its response to these environments, we tabulated genes that are up-regulated within macrophages (17) or under acid stress (18) but down-regulated in $\Delta mtrB$ (compared with the WT) grown *in vitro*. 101 genes (Table S1), which are induced upon infection of macrophages by *M. tuberculosis*, were down-regulated in $\Delta mtrB$ grown *in vitro*, and 32 genes (Table S2) that are part of the *M. tuberculosis* acid response were also down-regulated in the mutant (Fig. 4C). This was in line with our observation that $\Delta mtrB$ was compromised in its ability to respond appropriately to acidic pH. Furthermore, of the set of *M. tuberculosis* genes deemed essential for growth (19, 20), 71 were down-regulated in $\Delta mtrB$ compared with the WT (Table S3).

To better understand the effects of *mtrB* deletion at system level, we integrated an existing protein–DNA (pd) network of *M. tuberculosis* (21) with the protein–protein (pp) interaction network obtained from the STRING database to create a static network of *M. tuberculosis* pd and pp interactions. The microarray data available to us was mapped onto this network, enabling us to visualize the dysregulation of genes and interactomes linked to *mtrB* deletion. Dysregulation of genes likely of relevance to bacterial fitness under hypoxia and in macrophages is discussed below.

The transcriptional response to hypoxia and macrophage infection

Network analysis showed that a number of interacting partners of MtrB were down-regulated in $\Delta mtrB$. The TCS DosR (RR)/DosS (SK) (also known as DevR/DevS) has been implicated in the initial response to hypoxia and in sensing NO, carbon monoxide, and acidic pH and for *M. tuberculosis* persistence in macaques (22, 23). A striking observation was the down-regulation of the *dosR* regulon in $\Delta mtrB$ (Figs. 4B and 5A). The majority of connections to DosR, including the pp connections, were down-regulated in $\Delta mtrB$ (Fig. S3A). We validated the down-regulation of several of these genes by qRT-

¹⁰ Please note that the JBC is not responsible for the long-term archiving and maintenance of this site or any other third party hosted site.



MtrB regulates mycobacterial survival in vivo

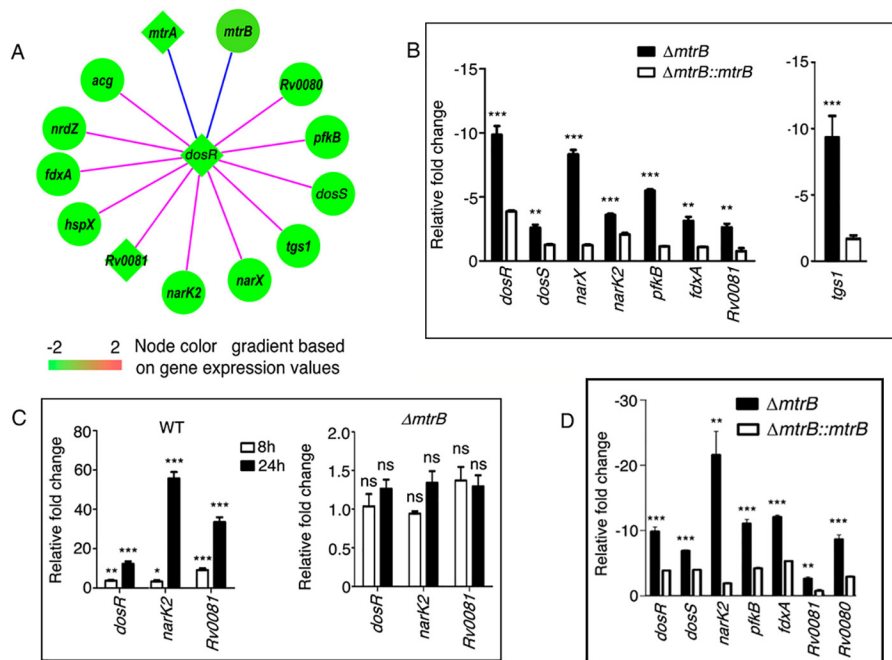


Figure 5. MtrB regulates expression of genes of the DosR regulon. *A*, network representation of the *dosR* regulon showing a subset of genes differentially regulated in $\Delta mtrB$. The blue edges denote protein–protein interactions; the pink edges denote protein–DNA interactions. Rectangular nodes represent transcription factors; circular nodes represent other proteins. The color scale of the nodes was assigned according to the \log_2 -fold change in gene expression in $\Delta mtrB$ compared with the WT (set as 1). *B*, relative expression of genes of the DosR regulon in $\Delta mtrB$ and $\Delta mtrB::mtrB$ compared with the WT under normoxia (set as 1). *C*, expression of DosR regulon genes after recovery from hypoxia analyzed at the indicated time intervals. *D*, expression of genes of the DosR regulon in *M. tuberculosis* strains after infection of macrophages. *C* and *D*, Error bars represent S.D., $n = 3$. *, $p < 0.05$; **, $p \leq 0.01$; ***, $p \leq 0.001$; ns, nonsignificant.

PCR (Fig. 5B). qRT-PCR of genes representative of the *dosR* regulon, namely *dosR*, *dosS*, *narX*, *narK2*, *pfkB*, *fdxA*, *Rv0081*, and *tgs1*, confirmed their down-regulation in $\Delta mtrB$ compared with the WT (Fig. 5B). This was reversed in $\Delta mtrB::mtrB$. These results were in conformity with the compromised survival of $\Delta mtrB$ under hypoxia. NarK2 is a H⁺/nitrate symporter, and *narX* is a part of the *narK2X* operon that is induced under hypoxia (24). *pfkB*, although encoding a putative phosphofructokinase, is reportedly devoid of phosphofructokinase activity (25). Its expression is enhanced upon hypoxia or growth arrest or in the intraphagosomal environment. *fdxA* encodes a ferredoxin and is induced at low pH (26) and in infected macrophages (27). Rv0081 is a transcriptional regulator that is part of an operonic locus under complex control (28). *In silico* modeling suggests that Rv0081 and Rv0082 could be responsible for communicating dormancy signals to the respiratory chain (29). Rv0081 is induced early during hypoxia and connects the early to the later hypoxic response by regulating the transcription factor Rv3334 (30). The biosynthesis of the major storage lipid triacylglycerol (TAG) depends on the TAG synthases *tgs1* and *tgs2* (31). *tgs1* is the principal TAG-synthesizing enzyme. Shi *et al.* (32) have reported that during growth arrest, there is a shift of carbon metabolism from providing biosynthetic precursors and energy to the synthesis of storage compounds such as TAG, which depends on *tgs1*. *tgs1* was down-regulated in $\Delta mtrB$ (Figs. 4B and 5B).

A large set of 230 genes is expressed at 4 and 7 days of hypoxia, constituting the “enduring hypoxic response” (33). Of these genes, 32 were down-regulated in $\Delta mtrB$ (Fig. S3B and Table S4), suggesting an inability of $\Delta mtrB$ to persist during long-term oxygen deprivation (Fig. 1H). 24 h after establishment of hypoxia, there was a striking increase in expression levels of *dosR*, *narK2*, and *Rv0081* in the WT (Fig. 5C, left panel) (compared with the expression levels before hypoxia) but not in $\Delta mtrB$ (Fig. 5C, right panel), raising the possibility that the inability to turn on the DosR regulon contributes at least in part to the inability of $\Delta mtrB$ to survive under hypoxia. Although DosR has been linked to the survival of *M. tuberculosis* under hypoxia, we noted that the levels of transcription of *dosR* under normoxic conditions were lower in $\Delta mtrB$ compared with the WT (Fig. 5B).

Rohde *et al.* (18) and Peterson *et al.* (34) have reported that *dosR* regulon genes are up-regulated early during infection of macrophages with *M. tuberculosis*, although this is unlikely to be due to environmental cues such as hypoxia, nitric oxide, or carbon monoxide. To decipher the role of MtrB in regulating the expression of DosR regulon genes during *in vitro* infection, we tested the expression of selected genes in bacteria residing in macrophages by qRT-PCR. We confirmed that $\Delta mtrB$ is compromised with respect to transcription of genes associated with the *dosR* regulon (*dosR*, *dosS*, *narK2*, *pfkB*, *fdxA*, *Rv0080*, and *Rv0081*) compared with the WT (Fig. 5D). These results sug-

Figure 4. MtrB is a global regulator of the *M. tuberculosis* transcriptome. *A*, pie chart representing the distribution of genes down-regulated in $\Delta mtrB$ grown *in vitro*. *B*, heat maps of differentially regulated genes grouped according to their Tuberculist functions or regulons. *C*, Venn diagrams representing the overlap between genes down-regulated in $\Delta mtrB$ and genes up-regulated in *M. tuberculosis* upon infection (left) or essential for growth of *M. tuberculosis* (middle) or up-regulated in *M. tuberculosis* under acid stress (right). The green arrow represents “down-regulated genes.”

gested that MtrB regulates transcription of DosR regulon genes that are possibly required for adaptation of the bacterium to the macrophage environment. These results were also in conformity with the compromised survival of $\Delta mtrB$ in macrophages (Fig. 2A).

In view of the above observations, we speculated that MtrB could potentially be involved in the transcription of basal levels of *dosR* under normoxia, possibly through physical interaction with DosR. To test whether DosR and MtrB interact physically, S-MtrB (cytosolic domain)-expressing *Escherichia coli* lysate was incubated with His-DosR (expressed in *E. coli*) immobilized on Ni²⁺-NTA-agarose. Bound proteins were positive for the presence of MtrB when analyzed by immunoblotting with S-antibody (Fig. 6A, last lane). As a negative control, lysates of *E. coli* expressing the cytosolic domain of another sensor kinase, KdpD (of the TCS KdpDE) (2), were incubated with immobilized His-DosR. No interaction was observed. We also tested for interaction between MtrB and DosR within mycobacteria using the mycobacterial protein fragment complementation (M-PFC) method. MtrB and DosR interacted when expressed in *M. smegmatis* (Fig. 6B). These results strengthened our view that MtrB interacts with DosR. To test whether these interactions regulate the DNA-binding ability of DosR, we performed electrophoretic mobility shift assays (EMSAs) to test the binding of DosR to an *hspX* promoter-derived DNA (35) in the absence or presence of MtrB. DosR (which had not been phosphorylated *in vitro*) did not show significant binding to *hspX* DNA at a concentration of 2.5 μ M. However, a mobility shift was clearly visible when DosR was incubated with varying concentrations of MtrB prior to use in EMSAs (Fig. 6C). These results suggested that by virtue of interacting with DosR, MtrB enhances the DNA-binding ability of DosR. MtrB alone did not bind to the *hspX* DNA (Fig. S3C). DosR is autoregulated and binds to its own promoter. Similar to the *hspX* promoter, MtrB could enhance the binding of DosR with its own promoter (Fig. S3D). The mutation H305A rendered MtrB kinase-inactive (Fig. S3E). This kinase-inactive mutant was able to enhance the binding of DosR to the *hspX* or the *dosR* promoter DNA in the same manner as the WT (Fig. S3, F and G), suggesting that the ability of MtrB to enhance DosR activity does not require the kinase activity of MtrB. *In vitro* pulldown (Fig. S3H) and M-PFC assays in the mycobacterial environment (Fig. S3I) confirmed that both the WT and the kinase-inactive mutant of MtrB interact with DosR. We contend that interaction of the cytosolic domain of MtrB with DosR is required for binding of DosR to DNA under normoxia in a phosphorylation-independent manner and subsequent survival of the bacterium under hypoxia.

The division cell wall (DCW) cluster, cell division, and peptidoglycan synthesis

Considering that the cells of $\Delta mtrB$ were increased in length compared with the WT, we searched the transcriptomic data for changes in expression of genes associated with cell division. The DCW cluster in *M. tuberculosis* includes essential cell division genes such as *ftsZ*, *ftsQ*, *ftsW*, *wag31*, and *sepF* and the *mur* enzymes that are required for peptidoglycan synthesis (36). These genes are required for cell wall homeostasis, cell division,

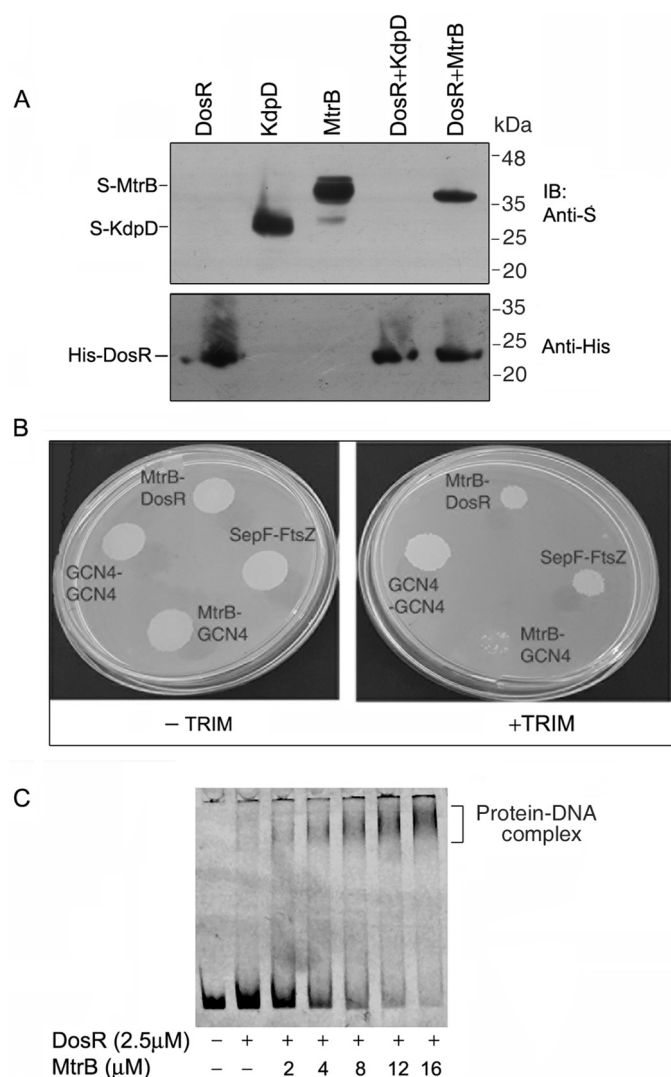


Figure 6. *M. tuberculosis* DosR interacts with MtrB and regulates DNA binding of DosR. A, S-MtrB (cytosolic domain)-expressing *E. coli* lysate (or KdpD (cytosolic domain)-expressing *E. coli* lysate as a negative control) was incubated with His-DosR (expressed in *E. coli*) immobilized on Ni²⁺-NTA-agarose. After washing the protein-bound resin, bound proteins were analyzed by immunoblotting (IB) with S-antibody and reprobed with His antibody. Lanes 1, 2, and 3, cell-free lysates of *E. coli* expressing His-DosR, S-KdpD, and S-MtrB (cytoplasmic domain), respectively; lanes 4 and 5, pulldowns of lysates expressing S-KdpD or S-MtrB, respectively, with DosR-bound Ni²⁺-NTA-agarose. B, M-PFC assay was used to determine association of DosR with MtrB. *M. smegmatis* expressing DosR fused to one half of murine DHFR and MtrB (cytosolic domain) fused to the other half of murine DHFR was grown in the absence or presence of TRIM. Plates were incubated at 37 °C for 7 days. Growth on TRIM indicated reconstitution of DHFR, which occurs when there is interaction between the protein pair. GCN4-GCN4 and SepF-FtsZ served as positive controls, and MtrB-GCN4 served as a negative control for protein-protein interaction. C, binding of DosR to the *hspX* promoter was analyzed by EMSA. EMSA was performed by incubating a Cy5-labeled PCR fragment derived from the *hspX* promoter with DosR in the absence or presence of different concentrations of MtrB. The reaction mixture was separated by PAGE, and the DNA-protein complex was visualized using a Typhoon biomolecular imager.

growth, and survival of *M. tuberculosis*. Microarray analysis (Fig. 4B) and qRT-PCR (Fig. 7A) showed that genes of the DCW cluster (*ftsZ*, *ftsQ*, and *ftsW*) were down-regulated in $\Delta mtrB$. *ilvE* encodes an enzyme that catalyzes the conversion of valine to alanine for peptidoglycan synthesis. It was down-regulated in $\Delta mtrB$ (Fig. 7A). Furthermore, the *mur* enzymes that catalyze

MtrB regulates mycobacterial survival in vivo

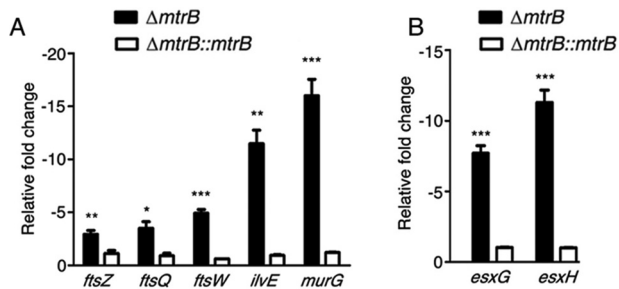


Figure 7. MtrB is required for expression of genes associated with peptidoglycan biosynthesis and lysosomal trafficking. A and B, relative expression of genes associated with peptidoglycan biosynthesis and cell division (A) or regulation of lysosomal trafficking (B) from $\Delta mtrB$ (filled bars) and $\Delta mtrB::mtrB$ (open bars) was quantitated by qRT-PCR. Gene expression is shown relative to that of the WT (set as 1). Error bars represent S.D., $n = 3$. ***, $p < 0.001$; **, $p < 0.01$; *, $p < 0.05$.

ligation and transferase reactions in peptidoglycan synthesis, namely *murC*, *murF*, *murG*, and *murX*, were down-regulated, as evidenced in the microarray data (Fig. 4B). The down-regulation of *murG*, the final enzyme in the peptidoglycan synthesis pathway, was validated by qRT-PCR (Fig. 7A). The slower growth rate and increased cell length of $\Delta mtrB$ are likely consequences of decreased expression of cell division and peptidoglycan-synthesizing genes. Previous studies have shown that transposon insertions in genes linked to cell wall synthesis render *M. tuberculosis* hypersusceptible to acid stress (37). The increased susceptibility of $\Delta mtrB$ to acid stress (Fig. 1G) was in harmony with the compromised expression of genes linked to cell wall synthesis. This effect was reversed in the *mtrB*-complemented strain.

Genes regulating lysosomal trafficking

M. tuberculosis harbors five chromosomal *esx* clusters that encode specialized type VII secretion systems (38). *esxG* and *esxH* are components of the ESX-3 secretion system. The ESCRT machinery is required to deliver *M. tuberculosis* to the lysosome. The EsxH–EsxG complex disrupts ESCRT function and impairs phagosome maturation (39). We observed from the microarray data that *esxG* and *esxH* were down-regulated (Fig. 4B) in $\Delta mtrB$ compared with the WT. This was confirmed by qRT-PCR (Fig. 7B). The attenuated expression of *esxG* and *esxH* likely accounts in part for the greater trafficking of $\Delta mtrB$ to the lysosome compared with the WT (Fig. 2C).

Discussion

One of the major challenges in the management of tuberculosis is the lack of detailed understanding of the players that enable the bacterium to evade immune surveillance mechanisms and to withstand the harsh environment prevailing within its host. In a recent study, Gorla *et al.* (40) reported the knockout of *mtrB* in *M. tuberculosis* only in the *MtrA*(Y102C) genetic background. In this study, we conclusively demonstrate that *mtrB* can be inactivated (even in the absence of *MtrA*(Y102C)) and that *MtrB* is not essential in *M. tuberculosis*. However, $\Delta mtrB$ was compromised in terms of its ability to survive in macrophages compared with the WT. It is known that *M. tuberculosis* inhibits phagosome maturation and prevents acidification of phagosomes harboring live bacilli as well

as their fusion with lysosomes. Recent reports suggest that *M. tuberculosis* survival and immune evasion are at least in part due to the suppression of autophagy and lysosomal trafficking. In line with this, a greater proportion of $\Delta mtrB$ colocalized with LC3 and LAMP1, markers of autophagosomes and lysosomes, respectively (Fig. 2). EsxH and EsxG in concert disrupt the function of the ESCRT machinery and hinder phagosome maturation (41). The down-regulation of *esxG* and *esxH* in $\Delta mtrB$ (Fig. 7B) is possibly linked to its diminished ability to subvert the host phagolysosomal fusion pathway and to survive in macrophages. We have therefore established that *ex vivo*, *MtrB* is required for subversion of the innate immune response, in terms of suppression of phagolysosomal trafficking of the bacterium. *In vivo*, bacterial cfu were much lower in the organs of mice infected with $\Delta mtrB$ compared with the WT (Fig. 3). These results suggest that the absence of *MtrB* attenuates the bacteria during *in vivo* infection. The inability to survive under acid stress and prevent phagolysosomal trafficking correlates directly with the attenuated phenotype of $\Delta mtrB$. This is in concordance with previous studies reporting the attenuated phenotype of mutants that are susceptible to acid stress (37). Furthermore, infection with $\Delta mtrB$ was characterized by a lack of immunopathology in the lungs of mice. This was in harmony with the decreased expression of *Tnf α* and *Il6* in the infected tissues. *TNF α* and IL-6 have been reported to be required for the initiation and maintenance of granuloma formation (42). To test whether the phenotype of $\Delta mtrB$ is associated with proinflammatory cytokine release from macrophages, we measured *TNF α* and IL-6 release from infected RAW264.7 cells. The release of the aforesaid cytokines was expectedly attenuated in the $\Delta mtrB$ -infected cells and restored upon complementation with *mtrB* (Fig. S2), strengthening the link between *MtrB* and the ability of *M. tuberculosis* to release cytokines involved in granuloma formation and the inflammatory response.

Considering that *M. tuberculosis* is exposed to a variety of stresses in its host, we tested the ability of $\Delta mtrB$ to withstand stress. We used the static culture hypoxia model described by McGillivray *et al.* (43) to test the role of *MtrB* in hypoxic survival. $\Delta mtrB$ was unable to survive under hypoxia, a characteristic that is partially restored in $\Delta mtrB::mtrB$ (Fig. 1H). *DosR* assists in maintaining metabolic homeostasis during hypoxia and enables recovery from dormancy (44, 45). The transition of *M. tuberculosis* to nonreplicating persistence is marked by induction of *DosR* genes and rerouting of carbon flux toward the synthesis of storage triacylglycerol. We observed by transcriptional profiling that *MtrB* is required for transcription of the *dosR* regulon under hypoxia, under normoxia, and in macrophages. This study therefore brings to light a hitherto unanticipated function of *MtrB* as a regulator of the *DosR* network. Interestingly, we demonstrated using pull-downs of recombinant *MtrB* from *E. coli* lysates with immobilized *DosR* that *MtrB* interacts directly with *DosR* (Fig. 6). This interaction was confirmed in the mycobacterial system as well. A phosphorylation-incompetent mutant of *MtrB*, H305A, was also able to interact with *DosR in vitro*. Vasisht *et al.* (46) have reported that phosphorylated *DosR* binds to the *hspX* promoter at a concentration of 0.5 μM , whereas nonphosphorylated *DosR* shows

weak binding even at a concentration of 3 μM . We have demonstrated that nonphosphorylated DosR did not show binding to the *hspX* promoter at a concentration of 2.5 μM . However, binding was clearly enhanced in the presence of MtrB (Fig. 6). In addition, we have demonstrated that the phosphorylation-incompetent MtrB mutant H305A was also capable of enhancing DosR binding to the *hspX* promoter, suggesting that the DosR–MtrB interaction enhances the DNA-binding ability of DosR in a phosphorylation-independent manner. We hypothesize that this interaction is possibly required for maintaining basal levels of DosR under normoxic conditions in a signal-independent manner. The underlying mechanism of MtrB-dependent binding of DosR to specific promoter regions remains to be elucidated. The *dosR*–*dosS* operon is autoregulated (47). DosR binds to its own promoter in a sequence-specific manner and regulates *dosR* promoter activity. Our results demonstrated that MtrB could augment DNA-binding ability of DosR to its own promoter in a phosphorylation-independent manner (Fig. S3). This binding is likely linked to the activation of the *dosR* regulon. It is plausible that binding of MtrB with DosR induces conformational changes in DosR that could enhance its DNA-binding ability, allowing maintenance of basal levels of DosR under normoxia when DosS is not active and DosR is not phosphorylated. In harmony with this, ΔmtrB was unable to launch a transcriptional response similar to the WT under hypoxia (Fig. 5C) and is compromised in its ability to activate the DosR regulon when grown in macrophages (Fig. 5D).

Another important observation is the inability of ΔmtrB to form biofilms (Fig. 1E). The growth of pathogens in organized biofilm-like structures in tissues promotes persistence. In the case of *M. tuberculosis*, biofilms are associated with a drug-tolerant phenotype (16, 48), rendering the inability of ΔmtrB to form biofilms particularly significant. The compromised production of ketomycolic acids in ΔmtrB possibly accounts, at least in part, to its inability to form biofilms. How MtrB regulates the synthesis of ketomycolic acids awaits further investigation. It has earlier been reported that the *pknG* mutant of *M. tuberculosis* is compromised in terms of its ability to survive under hypoxia or to form biofilms and at the same time shows an attenuated phenotype in an animal model and a compromised ability to elicit granuloma formation (49). Therefore, the inability of ΔmtrB to form biofilms or to survive under hypoxia is likely linked to the attenuated phenotype of ΔmtrB . MtrA(Y102C) is a gain-of-function mutant of MtrA, which functions in the absence of MtrB. We observed that complementation of ΔmtrB with *mtrA*(Y102C) did not restore biofilm formation. Based on these observations, we suggest that besides its role as the cognate sensor kinase of MtrA, MtrB also exerts phosphorylation-independent functions of significance to global regulation of the *M. tuberculosis* transcriptome. Along somewhat similar lines, it has previously been reported that MtrB regulates the cellular localization of Wag31 in a phosphorylation-independent manner (5).

Cell wall homeostasis is impaired in *mtrB*-inactivated mutants of *Mycobacterium avium* (10). In *Corynebacterium glutamicum*, MtrB plays an important role in maintaining cell shape and morphology (11). Here, we show compromised expression of genes linked to peptidoglycan synthesis and cell

division in ΔmtrB (Fig. 7A), which is likely linked to altered cell length of ΔmtrB compared with the WT. These are likely to reduce bacterial fitness under stress.

In conclusion, our study highlights a novel role of MtrB as an important regulatory hub in the *M. tuberculosis* gene expression network that controls the ability of *M. tuberculosis* to (a) respond to hypoxia, (b) subvert phagolysosomal trafficking, (c) form biofilms, (d) maintain cell wall homeostasis, and (e) regulate mycolate synthesis. We suggest that the regulation of these processes by MtrB is intimately linked to the ability of *M. tuberculosis* to infect mice because ΔmtrB was compromised in its ability to establish infection *in vivo*. The inability of ΔmtrB to survive under hypoxia suggests that MtrB is likely to be critical for persistence of *M. tuberculosis* within the host. Therefore, our studies bring to light the possibility of targeting MtrB for the development of novel therapeutics for the management of tuberculosis.

Materials and methods

Strains and growth conditions

M. tuberculosis H37Rv was grown in Middlebrook 7H9 medium containing 0.05% Tween 80 and 10% bovine albumin, dextrose, and catalase (ADC) (Difco) unless specified otherwise. The *mtrB* deletion strain (ΔmtrB) and the complemented strain ($\Delta\text{mtrB}::\text{mtrB}$) were grown in the same medium containing 20 $\mu\text{g}/\text{ml}$ kanamycin or 20 $\mu\text{g}/\text{ml}$ kanamycin plus 50 $\mu\text{g}/\text{ml}$ hygromycin B, respectively.

Inactivation of *mtrB*

The inactivation of *mtrB* was carried out in *M. tuberculosis* H37Rv using specialized transducing mycobacteriophages for allelic exchange. We inactivated *mtrB* by cloning 800-bp regions upstream (primers P1 and P2) and downstream (primers P3 and P4) of the gene into pYUB854Kan, ligating the construct to phAE159 to generate the allelic exchange substrate, and delivered the substrate by specialized transducing mycobacteriophages as described previously (50). The hygromycin cassette in pYUB854 was replaced with a kanamycin cassette from pMV261. Double crossovers were selected on 7H11 plates containing kanamycin. Positive colonies were verified by PCR amplifying a region 200 bp upstream and downstream of *mtrB* (primers P5 (A1) and P6 (A2)) and the kanamycin cassette (primers P7 (B1) and P8 (B2)). Southern blotting confirmed the deletion. The *mtrB*-complemented strain ($\Delta\text{mtrB}::\text{mtrB}$) was generated by cloning the WT full-length *mtrB* in pMV306 (Hyg+) and introducing the construct into the ΔmtrB strain. The list of primers is provided in Table S5.

His-tagged *mtrA*(Y102C) was generated as described previously (51). Control vector pLAM12 or *mtrA*(Y102C)::pLAM12 was electroporated separately into ΔmtrB . WT, ΔmtrB , or $\Delta\text{mtrB}::\text{mtrB}$ was grown to midexponential phase at 37 °C in Middlebrook 7H9 broth with appropriate antibiotics followed by induction with acetamide. Cultures were harvested and lysed in PBS containing protease inhibitor mixture (Cell Signaling Technology) in a mini bead beater. Proteins were solubilized in buffer containing 1% (v/v) Triton X-100 for 4 h at 4 °C with shaking. Expression of His-MtrA(Y102C) or MtrB was confirmed by Western blotting bacterial lysates with anti-His

MtrB regulates mycobacterial survival in vivo

(Abcam) or anti-MtrB (raised in our laboratory) antibody, respectively.

Aggregation and colony morphology

To test the aggregation phenotype, *M. tuberculosis* was grown in MB 7H9 containing 0.1% Tween 80 and 10% ADC to late log phase and left standing for 10 min at room temperature. For colony morphology, log-phase cultures were spotted on Dubos agar and allowed to grow for 4 weeks.

Biofilm formation

Log-phase cultures of *M. tuberculosis* strains were diluted 1:100 in 5 ml of Sauton's medium without detergent in T25 nonvented tissue culture flasks. The caps were wrapped in Parafilm, and flasks were incubated at 37 °C for 6 weeks as described by Ojha *et al.* (52). Caps were loosened after 4 weeks of incubation to facilitate biofilm growth. After 6 weeks, media below the biofilms were aspirated with a Pasteur pipette, and the film was allowed to dry. Crystal violet was added to the films and washed with water followed by reconstitution in alcohol after 15 min. Absorbance at 595 nm was measured to quantify the stain in the supernatant of each sample.

Mycolic acid isolation and analysis

Log-phase cultures were harvested and dried, and cells (50 mg) were treated with 40% tetrabutylammonium hydroxide (Merck) at 100 °C overnight. The mixture was cooled to room temperature. 2 ml of dichloromethane and 300 μ l of methyl iodide (Merck) were added, and the mixture was rotated at room temperature for 1 h. Phase separation was carried out by centrifugation at $1,400 \times g$ for 2 min. The aqueous phase was removed, and the organic phase was washed first with 2 ml of 3 N HCl followed by two washes with 2 ml of water. The organic phase was removed and dried followed by reconstitution in dichloromethane. Mycolic acid methyl esters were analyzed by TLC using petroleum ether:diethyl ether (95:5, v/v) six times. TLC plates were developed by charring after spraying with 20% (v/v) methanolic H₂SO₄.

Macrophage infections

BMDMs were prepared from the bone marrow obtained from the femora of BALB/c mice by culturing in Iscove's modified Dulbecco's medium containing 10% fetal bovine serum and macrophage colony-stimulating factor at 37 °C with 5% CO₂ until differentiation was complete. Infections were carried out at an m.o.i. of 10 for 4 h followed by treatment with gentamycin for 2 h.

Immunofluorescence microscopy

For colocalization experiments, bacteria were labeled with 100 μ g/ml FITC at 4 °C overnight. BMDMs were infected with FITC-labeled bacteria at an m.o.i. of 10 on coverslips. At the end of each infection, cells were fixed with 4% (v/v) paraformaldehyde for 10 min at 25 °C followed by permeabilization with 0.01% Triton X-100 in PBS for 10 min. The cells were then treated with 2% BSA in PBS for 90 min followed by treatment with either anti-LC3 antibody (MBL International) or anti-LAMP1 antibody (Abcam) overnight at 4 °C. Cells were treated

with Alexa Fluor 546–conjugated goat anti-rabbit antibody (Abcam), and coverslips were mounted with Slowfade (Thermo Scientific). Slides were imaged by confocal microscopy.

Animal infections

All mouse experiments were approved by the institutional Animal Ethics Committees of the National JALMA Institute, Agra, India, and the Bose Institute, Kolkata, India. BALB/c mice were purchased from Central Drug Research Institute, Lucknow, India and infected with aerosolized *M. tuberculosis* at the National JALMA Institute for Leprosy and Other Mycobacterial Diseases, Agra, India. Successful infection was confirmed by determination of cfu from the lungs of mice on Day 1. Each dose was \sim 100 cfu. Mice were sacrificed after 0, 4, 12, and 14 weeks of infection, and cfu were determined from the lungs and spleen. Lungs, after 4 weeks of infection, were homogenized in TRIzol, and RNA was isolated using the miRVANA RNA isolation kit (Ambion) following the manufacturer's protocol. For histopathology, infected lungs after 12 weeks were fixed in formalin, embedded in paraffin, and stained with hematoxylin and eosin. Sections were analyzed by a certified pathologist having no knowledge of the sample sets.

Microarray analysis

RNA was isolated from *M. tuberculosis* using the Qiagen RNA isolation kit. Labeling was carried out using Agilent's Quick Amp kit (cDNA synthesis and *in vitro* transcription) for 500 ng of RNA. Microarray-based gene expression profiling was carried out on an Agilent platform (8 \times 15,000 format). Microarray data analysis, normalization of data, and statistical analysis were carried by Genotypic Technology Pvt. Ltd., Bangalore, India using Agilent Genespring GX and Genotypic Biointerpreter database. Log₂ -fold change cutoff for up- or down-regulated genes was set to 0.8. Gene expression changes in the mutant greater than or equal to 0.8-fold of the WT were considered up-regulation, and changes less than or equal to -0.8 -fold of WT were considered down-regulation.

Networks and heat maps

The *M. tuberculosis* transcription factor network was obtained from Minch *et al.* (21). The pp interaction data were obtained from the STRING v10 (53) database online. These two data sets were merged to form a larger *M. tuberculosis* interaction network containing both protein–DNA and protein–protein interactions. The microarray data were integrated into this network, and regulons that displayed marked dysregulation were illustrated with Cytoscape v2.8.3 (54). The blue connections represent pp interactions, whereas the red connections show pd interactions. Diamond-shaped nodes indicate transcription factors, and elliptical nodes represent other proteins. The color of each node defines the expression level of that gene in the microarray data and ranges from red (high) to green (low). Heat maps were generated using the “heatmap.2” function of the “gplots” package in R, with the color gradient from green (low) to red (high).

RNA isolation from intracellular bacteria

RNA was prepared from intracellular *M. tuberculosis* following the method of Rohde *et al.* (18). Briefly, RAW264.7 cells

were seeded at 10^7 cells/T75 flask in four flasks for each strain of *M. tuberculosis*. The cells were infected at an m.o.i. of 10 for 4 h followed by treatment with gentamycin for another 2 h to remove extracellular bacteria. The cells were then washed with PBS and lysed in guanidinium thiocyanate buffer containing *N*-lauryl sarcosine, sodium citrate, and β -mercaptoethanol. Lysates were centrifuged, and pelleted bacteria were washed with PBS containing 0.1% Tween 80. The pellet was lysed by the addition of lysozyme and TRIzol followed by bead beating. RNA was prepared by chloroform extraction followed by application to an RNeasy kit column (Qiagen). RNA was treated with DNase and quantified.

RNA isolation and qRT-PCR

Cell pellets were harvested from growing cultures, reconstituted in a lysis buffer containing guanidinium thiocyanate and β -mercaptoethanol, and lysed using a bead beater. RNA was prepared following the method of Rustad *et al.* (55). The lysate was centrifuged at high speed for 15 min followed by purification of RNA from the supernatant using the Qiagen RNeasy kit following the manufacturer's protocol. RNA was treated with Turbo DNase (Ambion) following the manufacturer's protocol. SYBR Green-based real-time PCR was carried out using the primers provided in Table S5. The relative expression of the target gene was normalized to the endogenous reference gene (16S rRNA). -Fold change was determined by the comparative C_T method.

Measurement of cytokines

Cytokine kits were purchased from Peprotech or Thermo Fischer Scientific. Cytokines were measured in the cell-free supernatants according to the manufacturers' instructions.

Cloning, expression, and purification of recombinant proteins

The cytosolic domain of MtrB encompassing amino acid residues Ser-234 to Gly-567 was cloned between EcoRI and HindIII in pET29a+ in-frame with an N-terminal S-tag using gene-specific primer pairs P15 and P16. The construct was verified by sequencing, transformed into *E. coli* BL21 (DE3), and then expressed with an S-tag by induction at 25 °C for 4 h with 250 μ M isopropyl 1-thio- β -D-galactopyranoside. Cells were harvested and lysed by freeze/thaw cycles, and cell-free lysates were used for further experiments. The recombinant His-tagged construct of the cytoplasmic domain of MtrB was a gift from Dr. Deepak Saini, Indian Institute of Science, Bengaluru, India, and the His-DevR (DosR)-expressing construct was a gift from Dr. Jaya Tyagi, All India Institute of Medical Sciences, New Delhi, India. MtrB and DosR were expressed in *E. coli* Origami (DE3) and *E. coli* C43 (DE3), respectively. Cells were harvested and lysed by freeze/thaw cycles, and His-tagged proteins were purified from cell-free supernatants chromatography on Ni²⁺-NTA-agarose.

In vitro pulldown assay

The interaction between the cytosolic domain of MtrB and DosR was tested as follows. *E. coli* lysate expressing His-DosR was incubated with Ni²⁺-NTA-agarose at 4 °C for 30 min. The slurry containing bound His-DosR was washed thoroughly fol-

lowed by incubation with *E. coli* lysate expressing S-tagged cytoplasmic domain or MtrB or with S-tagged KdpD (a nonspecific negative control) at 22 °C for 1 h. The slurry was washed thoroughly with wash buffer containing 30 mM imidazole, boiled in SDS gel denaturing buffer, and loaded on SDS-polyacrylamide gels. The separated proteins were electroblotted onto polyvinylidene difluoride membranes, immunoblotted with horseradish peroxidase-conjugated S-tag antibody (Novagen) followed by development with LumiGLO (Cell Signaling Technology) to detect agarose-bound S-tagged protein. Blots were re-probed with His antibody.

M-PFC assay

Protein interactions were analyzed in *M. smegmatis* using the M-PFC assay (56). The GCN4 homodimerization domain (fused to the N terminus of dihydrofolate reductase (DHFR)) was excised from the episomal plasmid pUAB100 or the integrative plasmid pUAB200 and replaced with DosR or MtrB (cytoplasmic domain), respectively. DosR was cloned between the BamHI and ClaI sites of pUAB100 using primers P17 and P18. MtrB was cloned between the MunI and ClaI sites of pUAB200 using primers P19 and P20. All constructs were verified by sequencing. Recombinant and control plasmids were separately electroporated in *M. smegmatis* and grown in Middlebrook 7H9 medium supplemented with 0.2% glycerol, 0.05% Tween 80, kanamycin, and hygromycin. Interacting clones were selected by spotting transformants on Middlebrook 7H11 medium containing 0.5% (w/v) glucose, kanamycin, hygromycin, and trimethoprim (TRIM) at a concentration of 20 μ g/ml.

EMSAs

The binding of DosR to the promoter of *hspX* or *dosR* was analyzed by EMSA. DNA fragments encompassing the upstream regions of *hspX* or *dosR* were PCR-amplified using appropriate primer pairs (Table S6) of which one was Cy5-labeled and genomic DNA of *M. tuberculosis* as a template. Binding of DosR with gel-purified PCR product (10 nM) was carried out in binding buffer (20 mM Tris/HCl, pH 8, 20 mM NaCl, 50 mM CaCl₂, 10 mM MgCl₂, 10 mM KCl, 5% glycerol, 0.05 mg of salmon sperm DNA/ μ l) for 30 min at 30 °C in a final volume of 10 μ l. Where mentioned, recombinant DosR was incubated with recombinant MtrB (cytosolic domain) at different concentrations in binding buffer for 30 min at 25 °C in a final volume of 10 μ l. Postincubation, protein mixtures were further incubated with gel-purified PCR product (10 nM) in binding buffer for another 30 min at 25 °C in a final volume of 20 μ l. The reaction mixtures were separated on 7% native polyacrylamide gels run in 0.5 \times Tris acetate/EDTA buffer at 4 °C and 120 V for 120 min. The protein-DNA complex was scanned on a Typhoon Trio Plus scanner (GE Healthcare).

In vitro kinase assay

Recombinant MtrB (WT or the mutant H305A) (15 μ M) was incubated with 1 μ Ci of [γ ³²P]ATP (3250 Ci/mmol; Board of Radiation and Isotope Technology, India) in kinase buffer (50 mM Tris/HCl, pH 8.0, 50 mM KCl, 10 mM MgCl₂) containing 50 μ M ATP at 30 °C for 60 min. Reactions were terminated by

MtrB regulates mycobacterial survival in vivo

adding 1× SDS-PAGE loading dye (2% SDS, 50 mM Tris/HCl, pH 6.8, 0.02% bromophenol blue, 1% β-mercaptoethanol, 10% glycerol). The samples were resolved by SDS-PAGE (12.5%). After electrophoresis, the gel was washed with distilled water and exposed to X-ray film for 1 h.

Hypoxia and acid stress

Hypoxia was established as described by McGillivray *et al.* (39). Briefly, *M. tuberculosis* strains were grown to log phase and transferred to T12.5 nonvented tissue culture flasks such that they were filled to the neck leaving ~1/8 volume free. The flasks were closed tightly, and the mouths were secured by Parafilm. One control flask containing methylene blue for each strain was also set up as an indicator of hypoxia. The flasks were incubated at 37 °C for 4–5 days before the methylene blue was completely discolored, marking day 0 of hypoxia, and cfu were assessed at the required time points. For acid stress, *M. tuberculosis* strains were grown in MB 7H9 containing 0.02% tyloxapol, pH 5.5, buffered with MES. cfu of all three strains were followed over a period of 6 days, and the percent reduction in cfu of cultures grown at pH 5.5 from that of cultures grown at pH 7.0 was plotted.

Statistical analysis

All statistical analyses were performed using GraphPad Prism v5. All data have been represented as means ± S.D., and Student's *t* test (two-tailed) was used for comparison of two groups.

Data availability

Data sets can be found in the NCBI Gene Expression Omnibus (GEO) under accession number GSE97958.

Ethics statement

Animal experiments were approved by the Institutional Animal Ethics Committee of National JALMA Institute for Leprosy and Other Mycobacterial Diseases, Agra India (IAEC/JALMA/55/2015) and Bose Institute, Kolkata, India (IAEC/BI/34/2015). All protocols adhered to the guidelines provided by the “Committee for the Purpose of Control and Supervision of Experiments on Animals” (CPCSEA), a statutory body of the Government of India, Ministry of Social Justice and Empowerment.

Author contributions—S. K. B., J. B., and M. Kundu conceptualization; S. K. B., D. S., S. S., J. B., and M. Kundu formal analysis; J. B. and M. Kundu supervision; J. B. and M. Kundu funding acquisition; S. K. B., S. L., A. K. S., and S. B. validation; S. K. B., S. L., A. K. S., S. B., M. Kumar, S. K. S., D. S., J. B., and M. Kundu investigation; S. K. B., S. L., A. K. S., S. B., P. G., and R. S. methodology; S. K. B., J. B., and M. Kundu writing—original draft; J. B. and M. Kundu project administration; K. J., U. D. G., P. G., and R. S. resources; R. S., M. Kundu, and J. B. writing—review and editing.

Acknowledgment—We thank Dr. Ashok Mukherjee for histopathological analysis.

References

1. Dorman, S. E., and Chaisson, R. E. (2007) From magic bullets back to the magic mountain: the rise of extensively drug-resistant tuberculosis. *Nat. Med.* **13**, 295–298 [CrossRef Medline](#)
2. Parish, T. (2014) Two-component regulatory systems of mycobacteria. *Microbiol. Spectr.* **2**, MGM2-0010-2013 [CrossRef Medline](#)
3. Zahrt, T. C., and Deretic, V. (2000) An essential two-component signal transduction system in *Mycobacterium tuberculosis*. *J. Bacteriol.* **182**, 3832–3838 [CrossRef Medline](#)
4. Plocinska, R., Purushotham, G., Sarva, K., Vadrevu, I. S., Pandeeti, E. V., Arora, N., Plocinski, P., Madiraju, M. V., and Rajagopalan, M. (2012) Septal localization of the *Mycobacterium tuberculosis* MtrB sensor kinase promotes MtrA regulon expression. *J. Biol. Chem.* **287**, 23887–23899 [CrossRef Medline](#)
5. Plocinska, R., Martinez, L., Gorla, P., Pandeeti, E., Sarva, K., Blaszczyk, E., Dziadek, J., Madiraju, M. V., and Rajagopalan, M. (2014) *Mycobacterium tuberculosis* MtrB sensor kinase interactions with FtsI and Wag31 proteins reveal a role for MtrB distinct from that regulating MtrA activities. *J. Bacteriol.* **196**, 4120–4129 [CrossRef Medline](#)
6. Dubrac, S., Boneca, I. G., Poupel, O., and Msadek, T. (2007) New insights into the WalK/WalR (YycG/YycF) essential signal transduction pathway reveal a major role in controlling cell wall metabolism, cell division and biofilm formation in *Staphylococcus aureus*. *J. Bacteriol.* **189**, 8257–8269 [CrossRef Medline](#)
7. Winkler, M. E., and Hoch, J. A. (2008) Essentiality, bypass, and targeting of the YycFG (VicRK) two-component regulatory system in Gram-positive bacteria. *J. Bacteriol.* **190**, 2645–2648 [CrossRef Medline](#)
8. Fukushima, T., Szurmant, H., Kim, E. J., Perego, M., and Hoch, J. A. (2008) A sensor histidine kinase co-ordinates cell wall architecture with cell division in *Bacillus subtilis*. *Mol. Microbiol.* **69**, 621–632 [CrossRef Medline](#)
9. Senadheera, M. D., Guggenheim, B., Spatafora, G. A., Huang, Y. C., Choi, J., Hung, D. C., Treglown, J. S., Goodman, S. D., Ellen, R. P., and Cvitkovitch, D. G. (2005) A VicRK signal transduction system in *Streptococcus mutans* affects *gtfBCD*, *gbpB*, and *fff* expression, biofilm formation, and genetic competence development. *J. Bacteriol.* **187**, 4064–4076 [CrossRef Medline](#)
10. Cangelosi, G. A., Do, J. S., Freeman, R., Bennett, J. G., Semret, M., and Behr, M. A. (2006) The two-component regulatory system mtrAB is required for morphotypic multidrug resistance in *Mycobacterium avium*. *Antimicrob. Agents Chemother.* **50**, 461–468 [CrossRef Medline](#)
11. Möker, N., Brocker, M., Schaffer, S., Krämer, R., Morbach, S., and Bott, M. (2004) Deletion of the genes encoding the MtrA-MtrB two-component system of *Corynebacterium glutamicum* has a strong influence on cell morphology, antibiotics susceptibility and expression of genes involved in osmoprotection. *Mol. Microbiol.* **54**, 420–438 [CrossRef Medline](#)
12. Bhatt, A., Fujiwara, N., Bhatt, K., Gurucha, S. S., Kremer, L., Chen, B., Chan, J., Porcelli, S. A., Kobayashi, K., Besra, G. S., and Jacobs, W. R., Jr. (2007) Deletion of *kasB* in *Mycobacterium tuberculosis* causes loss of acid-fastness and subclinical latent tuberculosis in immunocompetent mice. *Proc. Natl. Acad. Sci. U.S.A.* **104**, 5157–5162 [CrossRef Medline](#)
13. Lenaerts, A. J., Hoff, D., Aly, S., Ehlers, S., Andries, K., Cantarero, L., Orme, I. M., and Basaraba, R. J. (2007) Location of persisting mycobacteria in a guinea pig model of tuberculosis revealed by r207910. *Antimicrob. Agents Chemother.* **51**, 3338–3345 [CrossRef Medline](#)
14. Satsangi, A. T., Pandeeti, E. P., Sarva, K., Rajagopalan, M., and Madiraju, M. V. (2013) *Mycobacterium tuberculosis* MtrAY102C is a gain-of-function mutant that potentially acts as a constitutively active protein. *Tuberculosis* **93**, S28–S32 [CrossRef Medline](#)
15. Ojha, A. K., Baughn, A. D., Sambandan, D., Hsu, T., Trivelli, X., Guerardel, Y., Alahari, A., Kremer, L., Jacobs, W. R., Jr., and Hatfull, G. F. (2008) Growth of *Mycobacterium tuberculosis* biofilms containing free mycolic acids and harbouring drug-tolerant bacteria. *Mol. Microbiol.* **69**, 164–174 [CrossRef Medline](#)
16. Sambandan, D., Dao, D. N., Weinrick, B. C., Vilchèze, C., Gurucha, S. S., Ojha, A., Kremer, L., Besra, G. S., Hatfull, G. F., and Jacobs, W. R., Jr. (2013) Keto-mycolic acid-dependent pellicle formation confers tolerance to drug-sensitive *Mycobacterium tuberculosis*. *MBio* **4**, e00222-13 [CrossRef Medline](#)
17. Kimmey, J. M., and Stallings, C. L. (2016) Bacterial pathogens versus autophagy: implications for therapeutic interventions. *Trends Mol. Med.* **22**, 1060–1076 [CrossRef Medline](#)

18. Rohde, K. H., Veiga, D. F., Caldwell, S., Balázsi, G., and Russell, D. G. (2012) Linking the transcriptional profiles and the physiological states of *Mycobacterium tuberculosis* during an extended intracellular infection. *PLoS Pathog.* **8**, e1002769 [CrossRef Medline](#)
19. Rohde, K. H., Abramovitch, R. B., and Russell, D. G. (2007) *Mycobacterium tuberculosis* invasion of macrophages: linking bacterial gene expression to environmental cues. *Cell Host Microbe* **2**, 352–364 [CrossRef Medline](#)
20. Sasseti, C. M., Boyd, D. H., and Rubin, E. J. (2003) Genes required for mycobacterial growth defined by high density mutagenesis. *Mol. Microbiol.* **48**, 77–84 [CrossRef Medline](#)
21. Minch, K. J., Rustad, T. R., Peterson, E. J., Winkler, J., Reiss, D. J., Ma, S., Hickey, M., Brabant, W., Morrison, B., Turkarslan, S., Mawhinney, C., Galagan, J. E., Price, N. D., Baliga, N. S., and Sherman, D. R. (2015) The DNA-binding network of *Mycobacterium tuberculosis*. *Nat. Commun.* **6**, 5829 [CrossRef Medline](#)
22. Mehra, S., Foreman, T. W., Didier, P. J., Ahsan, M. H., Hudock, T. A., Kisse, R., Golden, N. A., Gautam, U. S., Johnson, A. M., Alvarez, X., Russell-Lodrigue, K. E., Doyle, L. A., Roy, C. J., Niu, T., Blanchard, J. L., et al. (2015) The DosR regulon modulate adaptive immunity and is essential for *Mycobacterium tuberculosis* persistence. *Am. J. Respir. Crit. Care Med.* **191**, 1185–1196 [CrossRef Medline](#)
23. Voskuil, M. I., Schnappinger, D., Visconti, K. C., Harrell, M. I., Dolganov, G. M., Sherman, D. R., and Schoolnik, G. K. (2003) Inhibition of respiration by nitric oxide induces a *Mycobacterium tuberculosis* dormancy program. *J. Exp. Med.* **198**, 705–713 [CrossRef Medline](#)
24. Sohaskey, C. D., and Wayne, L. G. (2003) Role of *narK2X* and *narGHJI* in hypoxic upregulation of nitrate reduction by *Mycobacterium tuberculosis*. *J. Bacteriol.* **185**, 7247–7256 [CrossRef Medline](#)
25. Phong, W. Y., Lin, W., Rao, S. P., Dick, T., Alonso, S., and Pethe, K. (2013) Characterization of phosphofructokinase activity in *Mycobacterium tuberculosis* reveals that a functional glycolytic carbon flow is necessary to limit the accumulation of toxic metabolic intermediates under hypoxia. *PLoS One* **8**, e56037 [CrossRef Medline](#)
26. Fisher, M. A., Plikaytis, B. B., and Shinnick, T. M. (2002) Microarray analysis of the *Mycobacterium tuberculosis* transcriptional response to the acidic conditions found in phagosomes. *J. Bacteriol.* **184**, 4025–4032 [CrossRef Medline](#)
27. Schnappinger, D., Ehrt, S., Voskuil, M. I., Liu, Y., Mangan, J. A., Monahan, I. M., Dolganov, G., Efron, B., Butcher, P. D., Nathan, C., and Schoolnik, G. K. (2003) Transcriptional adaptation of *Mycobacterium tuberculosis* within macrophages: insights into the phagosomal environment. *J. Exp. Med.* **198**, 693–704 [CrossRef Medline](#)
28. He, H., Bretl, D. J., Penoske, R. M., Anderson, D. M., and Zahrt, T. C. (2011) Components of the Rv0081-Rv0088 locus, which encodes a predicted formate hydrogenlyase complex, are coregulated by Rv0081, MprA, and DosR in *Mycobacterium tuberculosis*. *J. Bacteriol.* **193**, 5105–5118 [CrossRef Medline](#)
29. Hegde, S. R., Rajasingh, H., Das, C., Mande, S. S., and Mande, S. C. (2012) Understanding communication signals during mycobacterial latency through predicted genome-wide protein interactions and Boolean modeling. *PLoS One* **7**, e33893 [CrossRef Medline](#)
30. Sun, X., Zhang, L., Jiang, J., Ng, M., Cui, Z., Mai, J., Ahn, S. K., Liu, J., Zhang, J., Liu, J., and Li, Y. (2018) Transcription factors Rv0081 and Rv3334 connect the early and the enduring hypoxic response of *Mycobacterium tuberculosis*. *Virulence* **9**, 1468–1482 [CrossRef Medline](#)
31. Daniel, J., Deb, C., Dubey, V. S., Sirakova, T. D., Abomoelak, B., Morbidoni, H. R., and Kolattukudy, P. E. (2004) Induction of a novel class of diacylglycerol acyltransferases and triacylglycerol accumulation in *Mycobacterium tuberculosis* as it goes into a dormancy-like state in culture. *J. Bacteriol.* **186**, 5017–5030 [CrossRef Medline](#)
32. Shi, L., Sohaskey, C. D., Pheiffer, C., Datta, P., Parks, M., McFadden, J., North, R. J., and Gennaro, M. L. (2010) Carbon flux rerouting during *Mycobacterium tuberculosis* growth arrest. *Mol. Microbiol.* **78**, 1199–1215 [CrossRef Medline](#)
33. Rustad, T. R., Harrell, M. I., Liao, R., and Sherman, D. R. (2008) The enduring hypoxic response to *Mycobacterium tuberculosis*. *PLoS One* **3**, e1502 [CrossRef Medline](#)
34. Peterson, E. J., Bailo, R., Rothchild, A. C., Arrieta-Ortiz, M. L., Kaur, A., Pan, M., Mai, D., Abidi, A. A., Cooper, C., Aderem, A., Bhatt, A., and Baliga, N. S. (2019) Path-seq identifies an essential mycolate remodelling program for mycobacterial host adaptation. *Mol. Syst. Biol.* **15**, e8584 [CrossRef Medline](#)
35. Chauhan, S., and Tyagi, J. S. (2008) Cooperative binding of phosphorylated DevR to upstream sites is necessary and sufficient for activation of the *Rv3134c-devRS* operon in *Mycobacterium tuberculosis*: implication in the induction of DevR target genes. *J. Bacteriol.* **190**, 4301–4312 [CrossRef Medline](#)
36. Hett, E. C., and Rubin, E. J. (2008) Bacterial growth and cell division: a mycobacterial perspective. *Microbiol. Mol. Biol. Rev.* **72**, 126–156 [CrossRef Medline](#)
37. Vandal, O. H., Roberts, J. A., Odaira, T., Schnappinger, D., Nathan, C. F., and Ehrt, S. (2009) Acid-susceptible mutants of *Mycobacterium tuberculosis* share hypersusceptibility to cell wall and oxidative stress and to the host environment. *J. Bacteriol.* **191**, 625–631 [CrossRef Medline](#)
38. Simeone, R., Bottai, D., and Brosch, R. (2009) ESX/type VII secretion systems and their role in host-pathogen interaction. *Curr. Opin. Microbiol.* **12**, 4–10 [CrossRef Medline](#)
39. Mehra, A., Zahra, A., Thompson, V., Sirisaengtaksin, N., Wells, A., Porto, M., Köster, S., Penberthy, K., Kubota, Y., Dricot, A., Rogan, D., Vidal, M., Hill, D. E., Bean, A. J., and Philips, J. A. (2013) *Mycobacterium tuberculosis* type VII secreted effector EsxH targets host ESCRT to impair trafficking. *PLoS Pathog.* **9**, e1003734 [CrossRef Medline](#)
40. Gorla, P., Plocinska, R., Sarva, K., Satsangi, A. T., Pandeeti, E., Donnelly, R., Dziadek, J., Rajagopalan, M., and Madiraju, M. V. (2018) MtrA response regulator controls cell division and cell wall metabolism and affects susceptibility of mycobacteria to the first line antituberculosis drugs. *Front. Microbiol.* **9**, 2839 [CrossRef Medline](#)
41. Tinaztepe, E., Wei, J. R., Raynowska, J., Portal-Celhay, C., Thompson, V., and Philips, J. A. (2016) Role of metal-dependent regulation of ESX-3 secretion in intracellular survival of *Mycobacterium tuberculosis*. *Infect. Immun.* **84**, 2255–2263 [CrossRef Medline](#)
42. Welsh, K. J., Abbott, A. N., Hwang, S.-A., Indrigo, J., Armitige, L. Y., Blackburn, M. R., Hunter, R. L., Jr., and Actor, J. K. (2008) A role for tumour necrosis factor- α , complement C5 and interleukin-6 in the initiation and development of the mycobacterial cord factor trehalose 6',6'-dimycolate induced granulomatous response. *Microbiology* **154**, 1813–1824 [CrossRef Medline](#)
43. McGillivray, A., Golden, N. A., and Kaushal, D. (2015) The *Mycobacterium tuberculosis* Clp gene regulator is required for *in vitro* reactivation from hypoxia-induced dormancy. *J. Biol. Chem.* **290**, 2351–2367 [CrossRef Medline](#)
44. Leistikov, R. L., Morton, R. A., Bartek, I. L., Frimpong, I., Wagner, K., and Voskuil, M. (2010) The *Mycobacterium tuberculosis* DosR regulon assists in metabolic homeostasis and enables rapid recovery from nonrespiring dormancy. *J. Bacteriol.* **192**, 1662–1670 [CrossRef Medline](#)
45. Schubert, O. T., Ludwig, C., Kogadeeva, M., Zimmermann, M., Rosenberger, G., Gengenbacher, M., Gillet, L. C., Collins, B. C., Röst, H. L., Kaufmann, S. H., Sauer, U., and Aebersold, R. (2015) Absolute proteome composition and dynamics during dormancy and resuscitation of *Mycobacterium tuberculosis*. *Cell Host Microbe* **18**, 96–108 [CrossRef Medline](#)
46. Vasisht, A., Prithvi Raj, D., Gupta, U. D., Bhat, R., and Tyagi, J. S. (2016) The α 10 helix of DevR, the *Mycobacterium tuberculosis* dormancy regulator, regulates its DNA binding and activity. *FEBS J.* **283**, 1286–1299 [CrossRef Medline](#)
47. Bagchi, G., Chauhan, S., Sharma, D., and Tyagi, J. S. (2005) Transcription and autoregulation of the *Rv3134c-devR-devS* operon of *Mycobacterium tuberculosis*. *Microbiology* **151**, 4045–4053 [CrossRef Medline](#)
48. Marrakchi, H., Lanéele, M. A., and Daffé, M. (2014) Mycolic acids: structures, biosynthesis and beyond. *Chem. Biol.* **21**, 67–85 [CrossRef Medline](#)
49. Khan, M. Z., Bhaskar, A., Upadhyay, S., Kumari, P., Rajmani, R. S., Jain, P., Singh, A., Kumar, D., Bhavesh, N. S., and Nandicoori, V. K. (2017) Protein kinase G confers survival advantage to *Mycobacterium tuberculosis* during latency-like conditions. *J. Biol. Chem.* **292**, 16093–16108 [CrossRef Medline](#)

MtrB regulates mycobacterial survival in vivo

50. Bardarov, S., Bardarov, S., Jr, Pavelka, M. S., Jr., Sambandamurthy, V., Larsen, M., Tufariello, J., Chan, J., Hatfull, G., and Jacobs, W. R., Jr. (2002) Specialized transduction: an efficient method for generating marked and unmarked targeted gene disruptions in *Mycobacterium tuberculosis*, *M. bovis* BCG and *M. smegmatis*. *Microbiology* **148**, 3007–3017 [CrossRef](#) [Medline](#)
51. Chatterjee, A., Sharma, A. K., Mahatha, A. C., Banerjee, S. K., Kumar, M., Saha, S., Basu, J., and Kundu, M. (2018) Global mapping of MtrA-binding sites links MtrA to regulation of its targets in *Mycobacterium tuberculosis*. *Microbiology* **164**, 99–110 [CrossRef](#) [Medline](#)
52. Ojha, A. K., Jacobs, W. R., Jr, and Hatfull, G. F. (2015) Genetic dissection of mycobacterial biofilms. *Methods Mol. Biol.* **1285**, 215–226 [CrossRef](#) [Medline](#)
53. Szklarczyk, D., Franceschini, A., Wyder, S., Forslund, K., Heller, D., Huerta-Cepas, J., Simonovic, M., Roth, A., Santos, A., Tsafou, K. P., Kuhn, M., Bork, P., Jensen, L. J., and von Mering, C. (2015) STRING v10: protein-protein interaction networks, integrated over the tree of life. *Nucleic Acids Res.* **43**, D447–D452 [CrossRef](#) [Medline](#)
54. Smoot, M. E., Ono, K., Ruscheinski, J., Wang, P. L., and Ideker, T. (2011) Cytoscape 2.8: new features for data integration and network visualization. *Bioinformatics* **27**, 431–432 [CrossRef](#) [Medline](#)
55. Rustad, T. R., Roberts, D. M., Liao, R. P., and Sherman, D. R. (2008) Isolation of mycobacterial RNA in *Mycobacteria Protocols* (Parish, T., and Brown, A. C., eds) pp. 13–21, Humana Press, New York
56. Singh, A., Mai, D., Kumar, A., and Steyn, A. J. (2006) Dissecting virulence pathways of *Mycobacterium tuberculosis* through protein-protein association. *Proc. Natl. Acad. Sci. U.S.A.* **103**, 11346–11351 [CrossRef](#) [Medline](#)
57. Kapopoulou, A., Lew, J. M., Cole, S. T. (2011) The MycoBrowser portal: a comprehensive and manually annotated resource for mycobacterial genomes. *Tuberculosis* **91**, 8–13 [CrossRef](#) [Medline](#)